European Journal of Pharmacology 703 (2013) 1–10

Contents lists available at SciVerse ScienceDirect

European Journal of Pharmacology

journal homepage: www.elsevier.com/locate/ejphar

Molecular and cellular pharmacology

Crocetin, a carotenoid derivative, inhibits retinal ischemic damage in mice

Fumiya Ishizuka [a], Masamitsu Shimazawa [a], Naofumi Umigai [b], Hiromi Ogishima [a], Shinsuke Nakamura [a], Kazuhiro Tsuruma [a], Hideaki Hara [a,*]

[a] Molecular Pharmacology, Department of Biofunctional Evaluation, Gifu Pharmaceutical University, 1-25-4 Daigaku-nishi, Gifu 501-1196, Japan
[b] Riken Vitamin Co., Ltd., 2-9-18 Misaki-cho, Chiyoda-ku, Tokyo 101-8370, Japan

ARTICLE INFO

Article history:
Received 5 October 2012
Received in revised form
4 February 2013
Accepted 7 February 2013
Available online 18 February 2013

Keywords:
Crocetin
MAPK
Oxidative stress
Retinal ischemia

ABSTRACT

Crocetin, an aglycone of crocin, is found both in the saffron crocus (*Crocus starus* L.) and in gardenia fruit (*Gardenia jasminoides* Ellis). We evaluated the protective effects of crocetin against the retinal ischemia induced by 5 h unilateral ligation of both the pterygopalatine artery (PPA) and the external carotid artery (ECA) in anesthetized mice. The effects of crocetin (20 mg/kg, p.o.) on ischemia/reperfusion-induced retinal damage were examined by histological, electrophysiological, and anti-apoptotic analyses. Data for anti-apoptotic analysis was obtained by terminal deoxynucleotidyl transferase dUTP nick end labeling (TUNEL) staining. Using immunohistochemistry and immunoblotting, the protective mechanism mediating the effects of crocetin was evaluated by examining crocetin's effects on the expression of 8-hydroxy-2-deoxyguanosine (8-OHdG; used as a marker of oxidative stress) and on phosphorylations of mitogen-activated protein kinases [MAPK; viz. extracellular signal-regulated protein kinases (ERK), c-Jun N-terminal kinases (JNK) and p38], and the redox-sensitive transcription factors nuclear factor-kappa B (NF-κB) and c-Jun. The histological analysis revealed that ischemia/reperfusion (I/R) decreased the cell number in the ganglion cell layer (GCL) and the thickness of inner nuclear layer (INL), and that crocetin inhibited GCL and INL. ERG measurements revealed that crocetin prevented the I/R-induced reductions in a- and b-wave amplitudes seen at 5 days after I/R. In addition, crocetin decreased the numbers of TUNEL-positive cells and 8-OHdG-positive cells, and the phosphorylation levels of p38, JNK, NF-κB, and c-Jun present in the retina after I/R. These findings indicate that crocetin prevented ischemia-induced retinal damage through its inhibition of oxidative stress.

1. Introduction

Retinal ischemia, which leads to irreversible neuronal cell death, is involved in many ocular diseases, such as ischemic optic neuropathies, diabetic retinopathy, rubeotic glaucoma, and ocular ischemic syndrome (Bucolo et al., 2009, 2012; Bucolo and Drago, 2011). Ocular ischemic syndrome is the name given to a variable spectrum of aggregated ocular signs and symptoms that result from chronic ocular hypoperfusion, usually secondary to severe carotid artery occlusion may involve amaurosis fugax, central retinal artery occlusion, or branch retinal artery occlusion. Severe carotid artery stenosis or occlusion related to atherosclerosis is a common cause of this syndrome. As yet, a therapeutic agent has not been developed for ocular ischemic syndrome. Recently, we reported a new murine retinal ischemic model in which both the pterygopalatine artery (PPA) and the external carotid artery (ECA) were ligated (Ogishima et al., 2011). The PPA supplies blood to the ophthalmic artery (Lelong et al. 2007). Although the anastomotic site between PPA and ECA has not been determined accurately, the ECA contributes to the vascular network between the PPA and the ophthalmic artery (Fig. 1A) (Tamaki et al., 2006). This animal model is useful both for the clarification of the pathologic mechanisms underlying ocular ischemic syndrome and for the evaluation of neuroprotective drugs that might be used to target that syndrome. In our previous study, we found that edaravone, a free-radical scavenger, prevented the retinal ischemic damage present in that model (Ogishima et al., 2011). We therefore hypothesized that oxidative stress is likely to be causally involved in ischemia/reperfusion (I/R)-induced retinal damage.

Crocetin is one of the major active compounds both in the saffron crocus (*Crocus starus* L.) and in gardenia fruit (*Gardenia jasminoides* Ellis) (Ichi et al., 1995; Li et al., 1999). In these plants, crocetin is estimated to be synthesized from zeaxanthin by enzymatic cleavage and then glycosylated to crocins. Crocetin exhibits a yellow color, and is an amphiphilic low-molecular weight carotenoid compound, as shown in Fig. 1. Crocetin has been used as an important spice and natural food colorant in various parts of world (Selim et al., 2000; Watanabe and Terabe, 2000). Crocetin and crocin have been reported to possess a number of biological activities, as exemplified by anti-oxidation (Yamauchi et al., 2011), anti-apoptosis (Ohno

* Corresponding author. Tel./fax: +81 58 230 8126.
E-mail address: hidehara@gifu-pu.ac.jp (H. Hara).

0014-2999/$ - see front matter © 2013 Elsevier B.V. All rights reserved.
http://dx.doi.org/10.1016/j.ejphar.2013.02.007

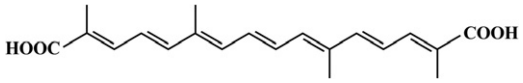

Fig. 1. Chemical structure of crocetin.

et al., 2012), anti-VEGF-induced angiogenesis (Umigai et al., 2012), anti-inflammatory (Hosseinzadeh and Younesi, 2002), anti-cancer (Wang et al., 1995), and hepatoprotective (Wang et al., 1991) effects, and by induced increases in retinal and choroidal blood flow (Xuan et al., 1999). Crocin has been shown to have a protective effect against the neuronal injury induced by occlusion of the middle cerebral artery (MCAO) in mice (Ochiai et al., 2007). However, the nothing is known about effects of crocetin in the model described above, in which retinal ischemia is induced in mice by ligation of the PPA and ECA.

In the present study, we used that model to examine the protective effects of crocetin orally administered against retinal cell death. To that end, we performed histological and electrophysiological analyses, and we also explored the underlying mechanism.

2. Materials and methods

2.1. Animals

Male ddY mice (Japan SLC, Hamamatsu, Japan), aged 8 to 9 weeks, were used in this study. They were kept under controlled lighting conditions (12 h: 12 h light/dark). All experiments were performed in accordance with the Association for Research in Vision and Ophthalmology Statement for the Use of Animals in Ophthalmic and Vision Research, and they were approved and monitored by the Institutional Animal Care and Use Committee of Gifu Pharmaceutical University.

2.2. Retinal ischemia model in mice

Anesthesia was induced by means of 2.0–3.0% isoflurane and maintained with 1.0–1.5% isoflurane (both in 70% N_2O/30% O_2), delivered using an animal anesthesia machine (Soft Lander; Sin-ei Industry Co. Ltd., Saitama, Japan). Body temperature was maintained at 37.0–37.5 °C with the aid of a temperature control system (NS-TC 10; Neuroscience Inc., Tokyo, Japan). Retinal ischemia was induced by PPA and ECA ligations, as described in our previous report (Ogishima et al., 2011). Briefly, after a midline skin incision the left common carotid artery was exposed, and the ECA was ligated. The internal carotid artery and its first branch were dissected, and the PPA was ligated (Fig. 2). Ischemia was maintained for 5 h, and then the ligatures were removed. All the above procedures were performed while the animal was under anesthesia.

2.3. Treatment with crocetin

Crocetin was prepared from extract of *G. Jasminoides* Ellis by Riken Vitamin Co., Ltd. (Tokyo, Japan). Briefly, the dried gardenia fruits which contained about 1.2% crocins (crocetin glycosides) were extracted with hydrous ethanol. Then, crocetin was prepared by hydrolyzation of the extracted crocins. The purity of crocetin was 78.9%. Crocetin was obtained from Riken Vitamin Co., Ltd. (Tokyo, Japan). It was suspended in distilled water containing 0.5% sodium carboxymethyl cellulose (CMC) immediately before use. Mice were treated orally either with crocetin at a dose of 20 mg/kg or with an identical volume (see below) of CMC. Each mouse received one of those treatments at 1 h before the ischemia, just after reperfusion, and at 6 and 12 h after the start of reperfusion, and then twice a day for the next 4 days. The injection volume was adjusted to 10 mL/kg body weight.

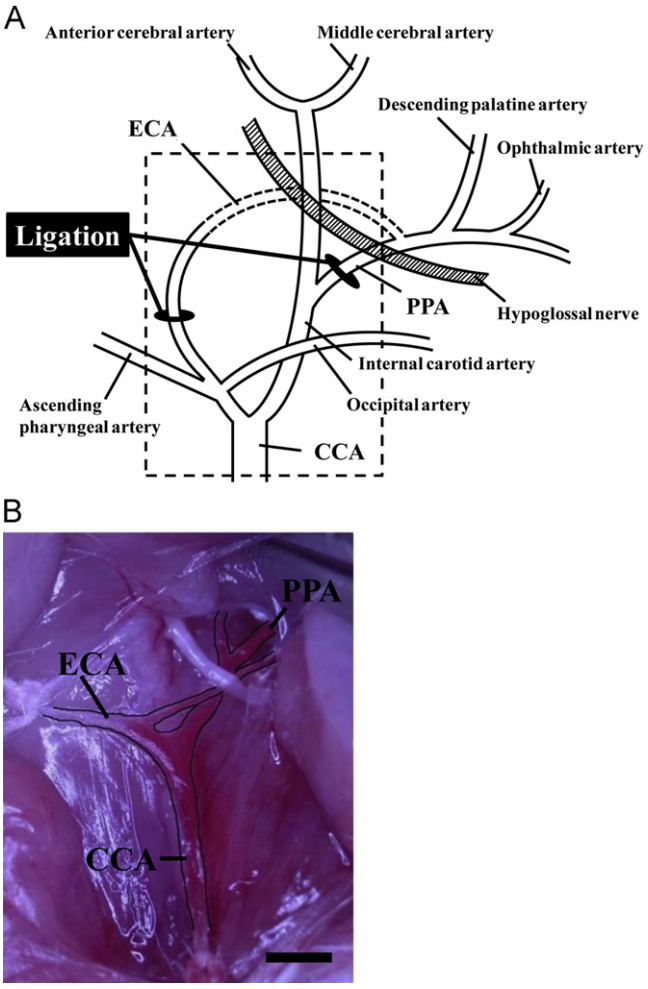

Fig. 2. The method for preparing of retinal ischemia model. (A) A illustration diagram showing vascular network leading from left ECA and PPA to retina, and the position of ligation. The square area enclosed by dot-line was shown in next photograph (B). (B) A photograph of the surgery showing ligation of left ECA. Scale bar represents 1 mm.

2.4. Electroretinogram (ERG) recording

ERG recordings were performed as in our previous report (Imai et al., 2010), at 5 days after the I/R. Scotopic ERG records were used to evaluate retinal function in mice that had been kept in a completely dark room for 24 h. They were anesthetized intraperitoneally with a mixture of ketamine (120 mg/kg; Daiichi-Sankyo, Tokyo, Japan) and xylazine (6 mg/kg; Bayer Health Care, Tokyo, Japan), and their pupils were dilated with 1% tropicamide and 2.5% phenylephrine (Santen Pharmaceutical Co., Ltd., Osaka, Japan). Flash ERG was recorded in the left eye of each dark-adapted mouse by placing a golden-ring electrode (Mayo, Aichi, Japan) in contact with the cornea and a reference electrode (Nihon Kohden, Tokyo, Japan) through the tongue. A neutral electrode (Nihon Kohden) was inserted subcutaneously near the tail. All procedures were performed in dim red light, and the mouse was mice were kept warm throughout the procedure. The amplitude of the a-wave was measured from the baseline to the highest a-wave peak, and the b-wave was measured from the highest a-wave peak to the highest b-wave peak.

2.5. Histology

Mice were euthanized under anesthesia after the ERG recordings. Left eyes were enucleated and kept immersed for at least 24 h at 4 °C in a fixative solution containing 4% paraformaldehyde. Eight paraffin-embedded sections (thickness, 5 μm) were cut through the optic disc parallel with the maximum circle of the eyeball. Following extraction of the eyeball, the top of the dorsal point was identified (using the optic axis as the landmark) and stained with hematoxylin and eosin. The damage induced by retinal ischemia was evaluated as described below, three sections from each eye being used for the morphometric analysis. On photographs of light-microscope images, the cell counts in the ganglion cell layer (GCL) between 375 and 625 μm from the optic disc (nasal and temporal portions), and the thickness of the inner plexiform layer (IPL) and that of the inner nuclear layer (INL) were measured at two points per section on the photographs. Those values were then averaged. Data from three sections were averaged for each eye and these values were entered into the analysis of the cell count in the GCL and the thickness of the IPL and of the INL.

2.6. TUNEL staining

Terminal deoxynucleotidyl transferase dUTP nick end labeling (TUNEL) was performed according to the manufacture's protocols (In Situ Cell Death Detection Kit; Roche Diagnostics, Mannheim, Germany) to assess the retinal cell death induced by retinal ischemia. Mice were euthanized by cervical dislocation at 24 h after ischemia. Eye were enucleated, kept immersed for at least 24 h at 4 °C in a fixative solution containing 4% paraformaldehyde, then immersed for 2 days in 25% sucrose with PBS, and finally embedded in a supporting medium for frozen tissue specimens (Optimum Cutting Temperature Compound; Tissue-Tek; Miles Laboratories, Naperville, IL, USA). Retinal sections were cut at 10 μm thickness on a cryostat at −25 °C, and stored at −80 °C until staining. After two washes with PBS, sections were incubated with terminal deoxyribonucleotidyl transferase enzyme at 37 °C for 1 h. Light-microscope images were photographed and labeled cells were counted in the GCL, INL, and outer nuclear layer (ONL) at a distance between 375 and 625 μm from the optic disc in two areas of the retina. The number of TUNEL-positive cells was averaged for these two areas, and the value so obtained was plotted as the number of TUNEL-positive cells for that eye.

2.7. Immunofluorescence staining

Mice were euthanized by cervical dislocation at 24 h after ischemia. Their eyes were enucleated, fixed overnight in 4% paraformaldehyde, and immersed for 2 days in 25% sucrose with PBS, then embedded in a supporting medium for frozen tissue specimens (Tissue-Tek). Retinal sections were cut at 10 μm-thickness on a cryostat at −20 °C, and stored at −80 °C until staining. Tissue sections were washed in 0.01 M PBS for 30 min, then preincubated with 10% normal goat serum in PBS for 1 h. The sections were then incubated overnight at 4 °C with 8-hydroxy-2-deoxyguanosine (8-OHdG) mouse mAb (Japan Institute for the Control of Aging, Shizuoka, Japan) in PBS. After washing with PBS, the sections were incubated for 1 h at room temperature with a mixture of an Alexa Fluor 488 $F(ab')_2$ fragment of rabbit anti-mouse IgG (H+L) (1:1000 dilution) (A11070; Invitrogen, Carlsbad, CA, USA). After a wash in PBS, the sections were incubated for 5 min in Hoechst 33342 (1:5000 dilution) (Invitrogen). The staining was evaluated by comparison with the negative control. Using a microscope (BX50; Olympus, Tokyo, Japan) fitted with a cooled charge-coupled device camera (DP30BP; Olympus), immunofluorescence images were obtained at 1360 × 1024 pixels with the aid of MetaMorph software (Molecular Devices, Sunnyvale, CA, USA), and on each image the 8-OHdG-positive cells were counted in the GCL, INL, and ONL at a distance between 375 and 625 μm from the optic disc.

2.8. Western blot analysis

Mice were euthanized by cervical dislocation, their eyeballs rapidly removed, and the retinas carefully separated from the eyeballs and quickly frozen in dry ice. For protein extraction, the tissue was homogenized in cell-lysis buffer using a Physcotron homogenizer (Microtec Co. Ltd., Chiba, Japan). The lysate was centrifuged at 12,000*g* for 20 min, and the supernatant was used for this study. The protein concentrations were measured by comparison with a known concentration of bovine serum albumin using a bicinchoninic acid protein assay kit (Pierce Chemical, Rockford, IL, USA). A mixture of equal parts of an aliquot of protein and sample buffer with 10% 2-mercaptoethanol was subjected to 15% sodium dodecyl sulfate-polyacrylamide gel electrophoresis. The separated protein was then transferred onto a polyvinylidene difluoride membrane (Immobilon-P; Millipore Corporation, Billerica, MA, USA). Transfers were blocked for 1 h at room temperature with 5% Block One-P (Nacalai Tesque Inc., Kyoto, Japan) in 10 mM Tris-buffered saline with 0.05% Tween 20, then incubated overnight at 4 °C with the primary antibody. For immunoblotting, the following primary antibodies were used: phosphorylated-p38 rabbit polyclonal antibody (Promega, Tokyo, Japan) (1:2000), phosphorylated-JNK rabbit polyclonal antibody (Cell Signaling, Danvers, MA, USA) (1:1000), phosphorylated-ERK rabbit monoclonal antibody (Cell Signaling) (1:1000), phosphorylated-c-Jun rabbit monoclonal antibody (Cell Signaling) (1:1000), phosphorylated-NF-κB rabbit polyclonal antibody (Cell Signaling) (1:1000), p38 rabbit polyclonal antibody (Cell Signaling) (1:1000), JNK rabbit polyclonal antibody (Santa Cruz Biotechnology, Santa Cruz, CA, USA) (1:1000), ERK rabbit polyclonal antibody (Cell Signaling) (1:1000), c-Jun rabbit monoclonal antibody (Cell Signaling) (1:1000), NF-κB rabbit polyclonal antibody (Cell Signaling) (1:1000), and β-actin mouse monoclonal antibody (Sigma-Aldrich, St. Louis, MO, USA) (1:5000). Goat anti-rabbit or anti-mouse horseradish peroxidase-conjugated (1:2000) was used as a secondary antibody. The immunoreactive bands were visualized using Immuno Star® LD (Wako Pure Chemical, Osaka, Japan), then measured using LAS-4000 Mini (Fuji Film Co., Ltd., Tokyo, Japan).

2.9. Statistical analysis

Data are presented as the means ± S.E.M. Statistical comparisons were made using a two-tailed student's *t* test or Dunnett's test by means of STATVIEW version 5.0 (SAS Institute, Cary, NC, USA). $P < 0.05$ was considered to indicate statistical significance.

3. Results

3.1. Crocetin protected against the histological damage in the mouse retina induced by I/R

I/R caused decreases in the cell number in the GCL and in the thickness of the IPL and that of the INL in the mouse retina [versus the control (no I/R) retina] at 5 days after ischemia. Oral administration of crocetin significantly prevented such reductions in the GCL cell number and INL thickness (versus the vehicle group) (Fig. 3A–C). Although crocetin tended to prevent the reduction in IPL thickness, the significance level was not reached (Fig. 3D).

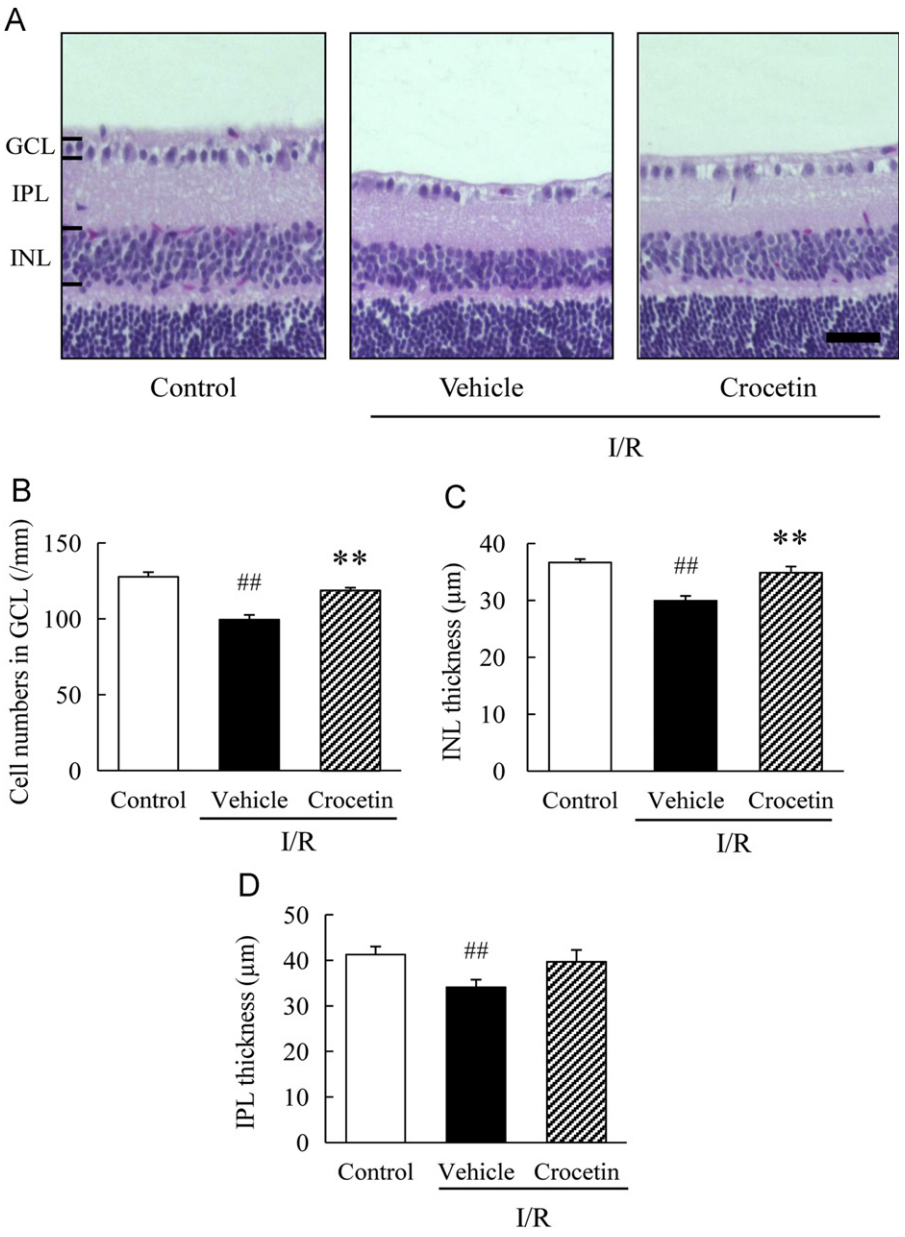

Fig. 3. Effects of crocetin on ischemia/reperfusion (I/R)-induced retinal morphological damage. (A) Representative photographs (hematoxylin and eosin staining of retinal sections) showing retinas treated with (a) CMC, (b) I/R plus vehicle, or (c) I/R plus crocetin. (B)–(D) Quantitative analysis of the cell number in GCL (B), and of the thickness of (C) INL and of (D) IPL, all at 5 days after I/R. Data are shown as means ± S.E.M. ($n=10$ to 12). $^{**}P<0.01$ vs. I/R plus vehicle (vehicle). $^{\#\#}P<0.01$ vs. CMC (control). Scale bar represents 50 μm.

3.2. Crocetin prevented the induction of cell apoptosis in the mouse retina following I/R

Terminal deoxynucleotidyl transferase dUTP nick-end labeling (TUNEL)-positive cells were observed in the GCL, INL, and ONL at 24 h after the onset of ischemia. Oral administration of crocetin significantly reduced the number of TUNEL-positive cells in GCL and INL (versus the vehicle-treated retina) (Fig. 4A–C), but had no effect on the number in ONL (Fig. 4D).

3.3. Crocetin inhibited functional damage in the mouse retina induced by I/R

The effects of crocetin on I/R-induced retinal degeneration were examined by means of electrophysiological analysis. In the control (no I/R) group, the a-wave and b-wave amplitudes were each increased in a light intensity-dependent manner. Each of these amplitudes was significantly reduced in the vehicle-treated group (versus the control group) at 5 days after I/R. The crocetin-treated group exhibited significant prevention of each compared with the vehicle-treated group (Fig. 5).

3.4. Crocetin prevented I/R-induced DNA oxidation in the mouse retina

The number of 8-OHdG-positive cells was increased in GCL, INL, and ONL at 24 h after the onset of ischemia. Crocetin reduced that number significantly in GCL and INL, but not in ONL (versus the vehicle group) (Fig. 6).

3.5. Crocetin prevented the I/R-induced activation of MAPK and redox-sensitive transcription factors in the mouse retina

This experiment investigated the mechanisms responsible for I/R-induced cell death in the retina and the effects of crocetin.

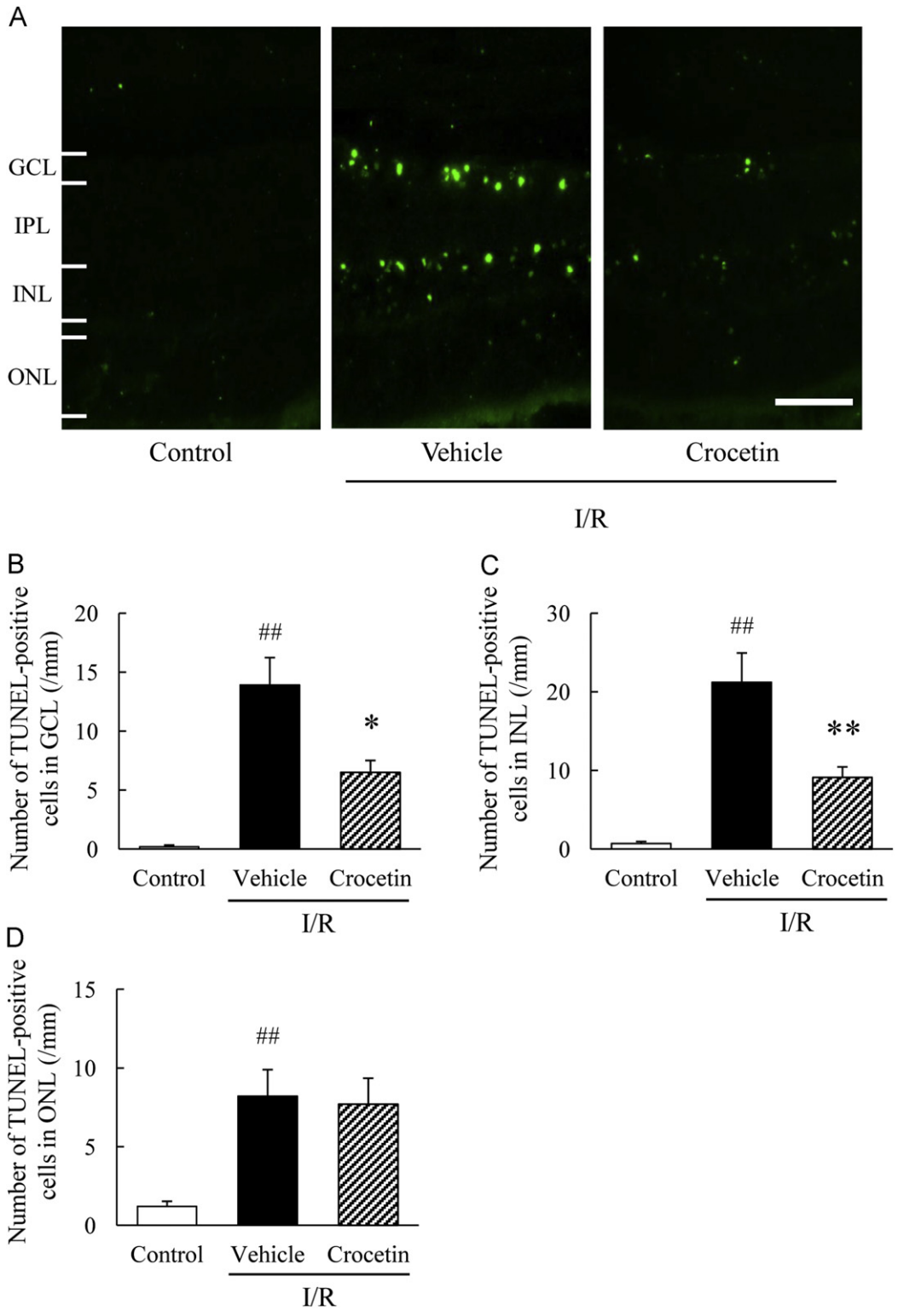

Fig. 4. Effects of crocetin on the retinal expression of TUNEL-positive cells at 24 h after the onset of ischemia. (A) Representative photographs showing retinas treated with (a) CMC, (b) I/R plus vehicle, or (c) I/R plus crocetin. (B)–(D) Quantitative analysis of the numbers of TUNEL-positive cells in (B) GCL, (C) INL, and (D) ONL. Data are shown as means ± S.E.M. ($n=10$). $^{*}P<0.05$, $^{**}P<0.01$ vs. I/R plus vehicle (vehicle). $^{\#\#}P<0.01$ vs. CMC (control). Scale bar represents 50 μm.

Levels of phosphorylated p38 and phosphorylated JNK were markedly increased (versus the control group) at 12 h after the onset of ischemia (expressed relative to total p38 and total JNK, respectively) (Fig. 7A–D). The ratio of phosphorylated ERK to total ERK was significantly increased (versus the control group) at 24 h after the onset of ischemia (Fig. 7E and F). Crocetin significantly reduced the I/R-induced phosphorylations of p38 and JNK (Fig. 7A–D), but not that of ERK (Fig. 7E and F).

The effects of crocetin on the I/R-induced activations of redox-sensitive transcription factors were evaluated by measuring the phosphorylations of c-Jun and NF-κB. The ratio of phosphorylated c-Jun to total c-Jun was significantly increased (versus the control

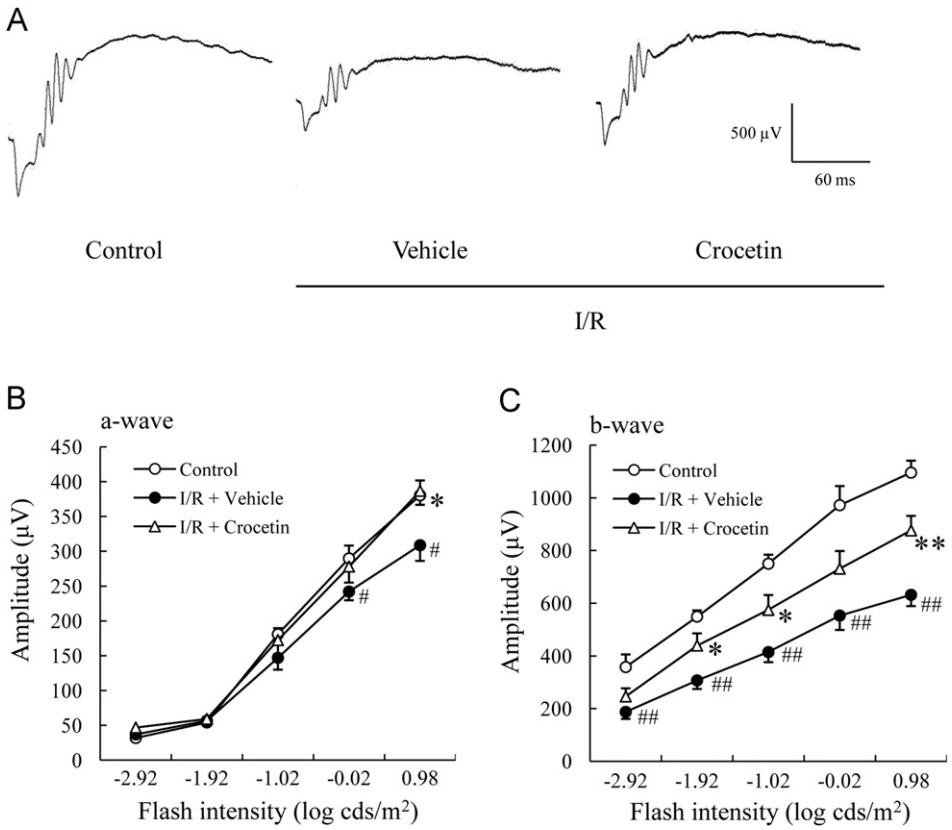

Fig. 5. Effects of crocetin on I/R-induced retinal functional damage. The effects of crocetin were evaluated by recording the electroretinogram (ERG) at 5 days after I/R. (A) Representative ERG recordings from retinas treated with CMC, I/R plus vehicle or I/R plus crocetin. Stimulus flashes were delivered at 0.98 log cd/m^2. (B) and (C) Intensity-response functions for dark-adapted (B) a-wave and (C) b-wave amplitudes. The crocetin-treated group showed significant preservation of both a- and b-wave amplitudes compared with the vehicle-treated group. Data are shown as means ± S.E.M. (n=9 to 12). $^{*}P<0.05$, $^{**}P<0.01$ vs. I/R plus the vehicle-treated group (vehicle). $^{\#}P<0.05$, $^{\#\#}P<0.01$ vs. CMC (control).

group) at 12 h after the onset of ischemia (Fig. 8A and B), while that of phosphorylated NF-κB to total NF-κB was significantly increased (versus the control group) at 24 h after the onset of ischemia (Fig. 8C and D). Crocetin significantly reduced each of these I/R-induced phosphorylations (Fig. 8).

4. Discussion

In the present study, oral administration of crocetin protected against I/R-induced retinal cell death and decreased the numbers of TUNEL-positive and 8-OHdG-positive cells in the retina. Crocetin also reduced the phosphorylations of MAPK, JNK, and p38, and those of the redox-sensitive transcriptional factors c-Jun and NF-κB in the mouse retina.

Neuronal cell death in the inner retina is induced by retinal I/R, which can be caused by such maneuvers as PPA and ECA ligation (Ogishima et al., 2011), increasing the intraocular pressure (Li et al., 2009), or central retinal artery occlusion (Goldenberg-Cohen et al., 2008). Furthermore, apoptosis is induced by retinal ischemia, and has been observed in the GCL, INL, and ONL following the retinal ischemia induced by ligation of PPA and ECA (Ogishima et al., 2011) and that induced by occlusion of the central retinal artery (Daugeliene et al., 2000). In the present study, the number of cells in GCL and the thickness of INL were decreased after ligation of PPA and ECA, while TUNEL-positivity, which is displayed by apoptotic cells, was increased in the retina. Administration of crocetin (20 mg/kg) inhibited not only the decrease in the number of cells in GCL and the decrease in INL thickness, but also the increases in TUNEL-positive cell numbers in GCL and INL. We previously measured plasma concentrations of crocetin in rats following oral administration at a dose of 10 mg/kg (Yamauchi et al., 2011). The plasma concentration was approximately 4.5 μM at 1 h after oral administration, which was a level sufficient to reduce in vitro cell death induced by H_2O_2 which is investigated in RGC-5 and SH-SY5Y cell lines (Yamauchi et al., 2011; Papandreou et al., 2011). Therefore, we administered crocetin at a dose of 20 mg/kg in the present study and administration at a dose of 20 mg/kg probably reached the effective concentration in retinal cells. In previous reports we demonstrated that in mice crocetin reduced the retinal cell death and apoptosis induced either by light exposure (Yamauchi et al., 2011) or by intravitreal administration of *N*-methyl-D-aspartate (NMDA) (Ohno et al., 2012), effects mediated by inhibitions of the activities of caspases. These findings revealed protective effects of crocetin against both retinal cell death and apoptosis.

Oxidative stress plays a crucial role in retinal ischemic injury, and the formation of reactive oxygen species (ROS) and free radicals during ischemia and after reperfusion triggers lipid peroxidation of membranes, denaturation of protein, and DNA damage (Kloner et al., 1989). Previously, we reported that edaravone, a free-radical scavenger, reduced the histological and functional retinal damage induced by ligation of PPA and ECA (Ogishima et al., 2011). Crocetin has been reported to have antioxidative effects in various experimental models, such as an in vitro H_2O_2-induced cell death model (Yamauchi et al., 2011), a hemi-parkinsonian rat model (Ahmad et al., 2005), a cardiac hypertrophy rat model (Shen et al., 2009), and a cerebral ischemic rat model (Yoshino et al., 2011). These findings indicate that crocetin has antioxidant activities, such as direct ROS scavenging

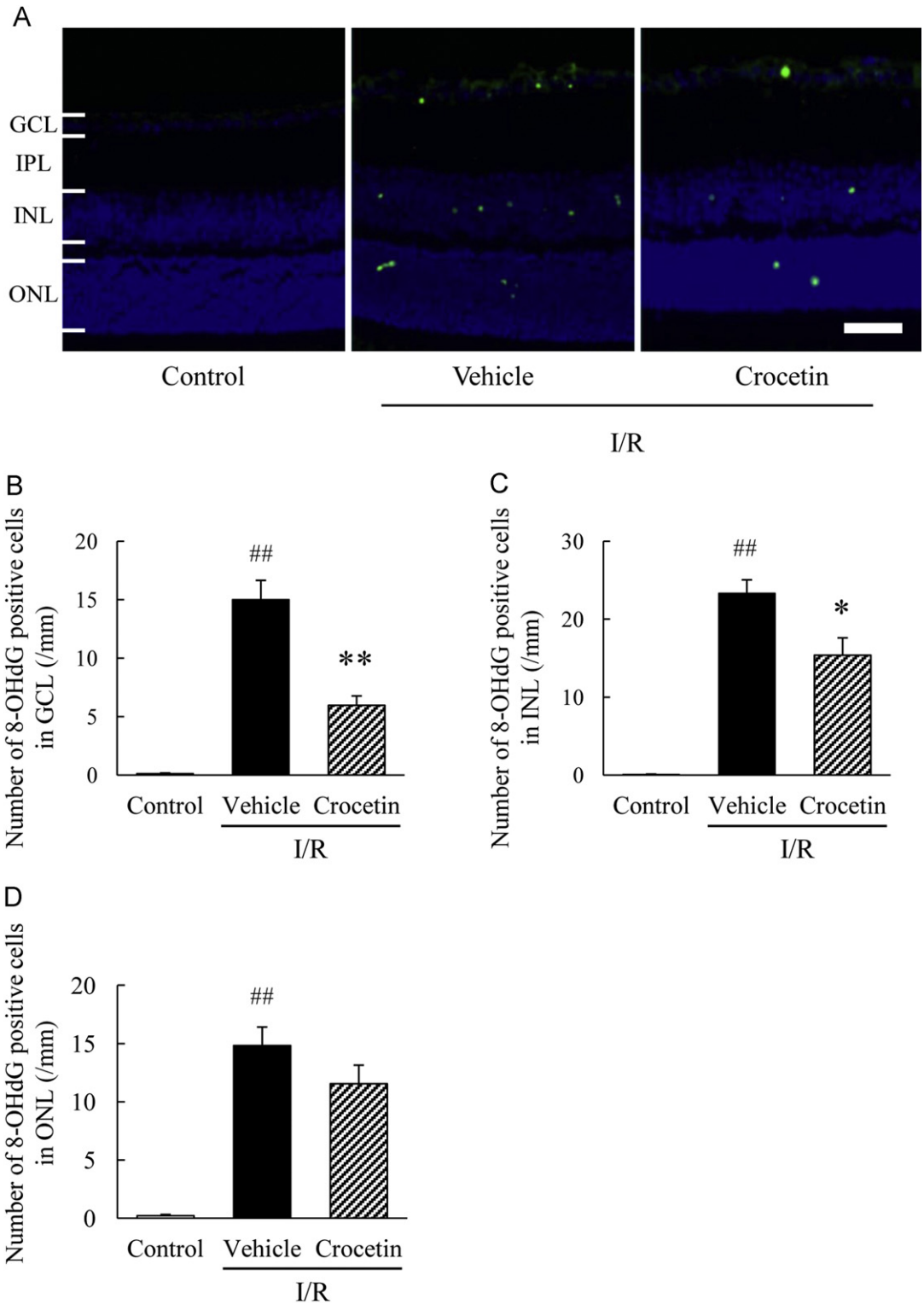

Fig. 6. Effects of crocetin on I/R-induced expression of 8-OHdG-positive cells at 24 h after the onset of ischemia. (A) Representative photographs of retinas treated with (a) CMC, (b) I/R plus vehicle, or (c) I/R plus crocetin. (B)–(D) Quantitative analysis of the numbers of 8-OHdG-positive cells in (B) GCL, (C) INL, and (D) ONL. Data are shown as means ± S.E.M. ($n=6$). $^{*}P<0.05$, $^{**}P<0.01$ vs. I/R plus vehicle (vehicle). $^{\#\#}P<0.01$ vs. CMC (control). Scale bar represents 50 μm.

(Yoshino et al., 2011) and stimulation of the activities of endogenous antioxidant enzymes (Shen and Qian, 2006). Therefore, to test whether the protective effects of crocetin against retinal ischemic damage might be caused at least partly by its antioxidative effects, we investigated the expression of a marker of oxidative stress, 8-OHdG. At 24 h after the onset of ischemia, 8-OHdG-positive cells were expressed in GCL, INL, and ONL, and the number of 8-OHdG-positive cells was significantly lower in the GCL and INL of the crocetin-treated group than in those layers of the vehicle-treated group. These results indicate that crocetin has a preventive effect against the oxidative stress induced by I/R.

According to various reports, both the a-wave and the b-wave of the ERG are reduced in amplitude after ischemia (Ogishima et al., 2011; Grozdanic et al., 2003). ERG recording is used as an

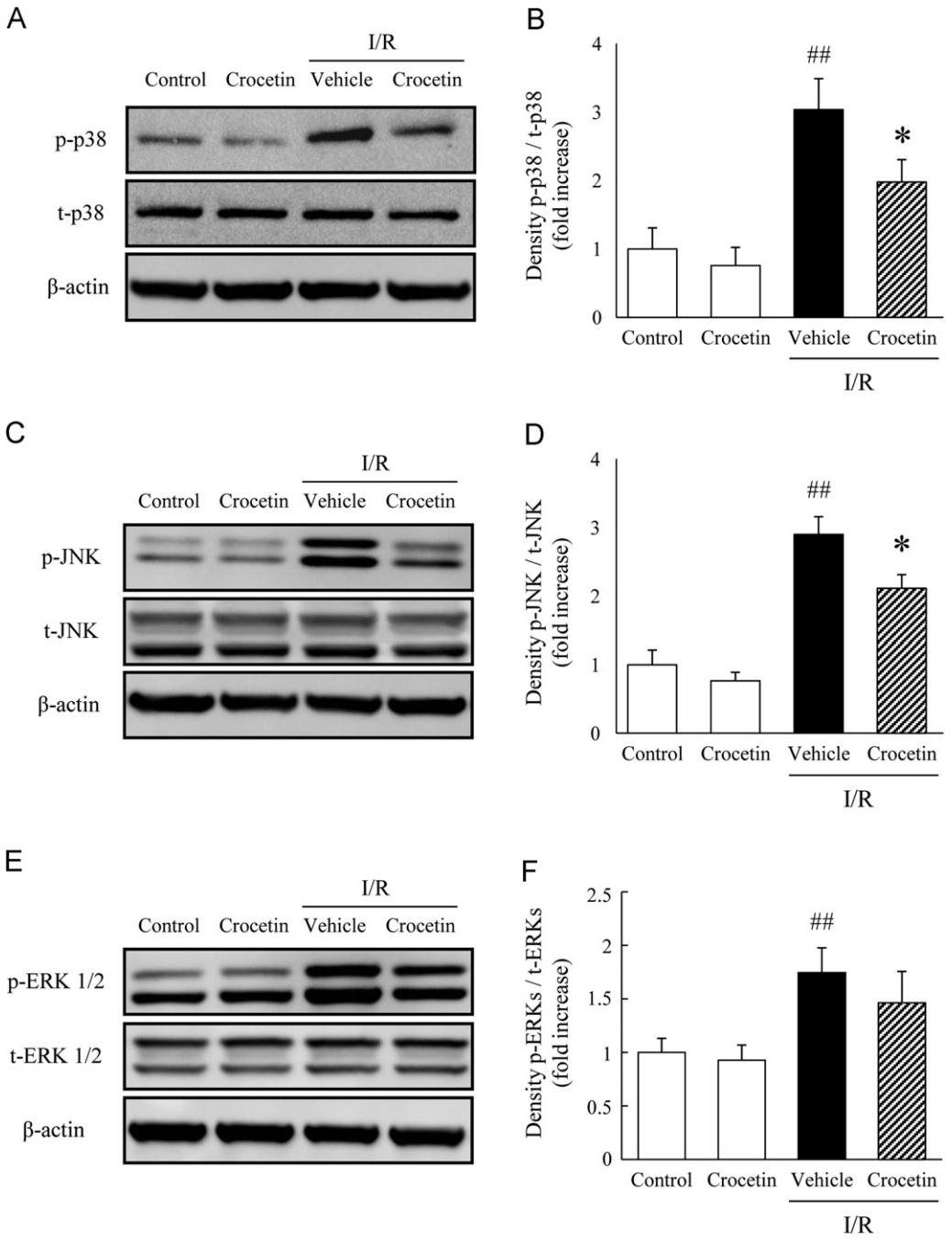

Fig. 7. Effects of crocetin on I/R-induced phosphorylation of MAPK in the mouse retina. (A), (C) and (E) Representative band images showing (A) p38, (C) JNK, and (E) ERK in retinas treated with CMC, crocetin, I/R plus vehicle, or I/R plus crocetin. (B), (D) and (F) Quantitative analysis of band densities for (B) p38, (D) JNK, and (F) ERK. Data are shown as means ± S.E.M. ($n=6$). $^{*}P<0.05$ vs. I/R plus vehicle group (vehicle). $^{\#\#}P<0.01$ vs. CMC group (control).

objective way of evaluating the functional status of the inner and outer retina, with the a-wave reflecting the function of the photoreceptors and the b-wave the functions of bipolar cells and Müller cells. After PPA and ECA ligation in the present mice, the amplitudes of both the a- and b-waves were reduced, and oral administration of crocetin protected against these reductions. The above findings illustrate that crocetin can attenuate the photoreceptor and inner retinal dysfunctions induced by I/R.

Multiple pathways are thought to play roles in the retinal cell death induced by oxidative stress. Antioxidants prevent activation of MAPK and redox-sensitive transcriptional factors (Wen et al., 2006; Yagi et al., 2009), and members of each major MAPK subfamily (JNK, p38, and ERK 1/2) have been implicated in the neuronal injury induced by retinal ischemia (Roth et al., 2003). In the present study, we investigated the I/R-induced phosphorylation of MAPKs (i.e., activation). We found that p38 and JNK activations peaked at 12 h after the onset of ischemia, while ERK activation was increased at 24 h after the onset of ischemia. p38 and JNK which are activated by various stresses, including ischemic and oxidative stresses are involved in cell differentiation and apoptosis (Xia et al., 1995), while ERK 1/2 is stimulated by oxidative stress and regulates cell proliferation and differentiation (Luo and DeFranco, 2006). Although the precise roles performed by ERK 1/2 are not clear, ERK 1/2 may, in some cases, not only promote cell survival, but also participate in neuronal cell death and neurodegeneration (Luo and DeFranco, 2006). Therefore, we

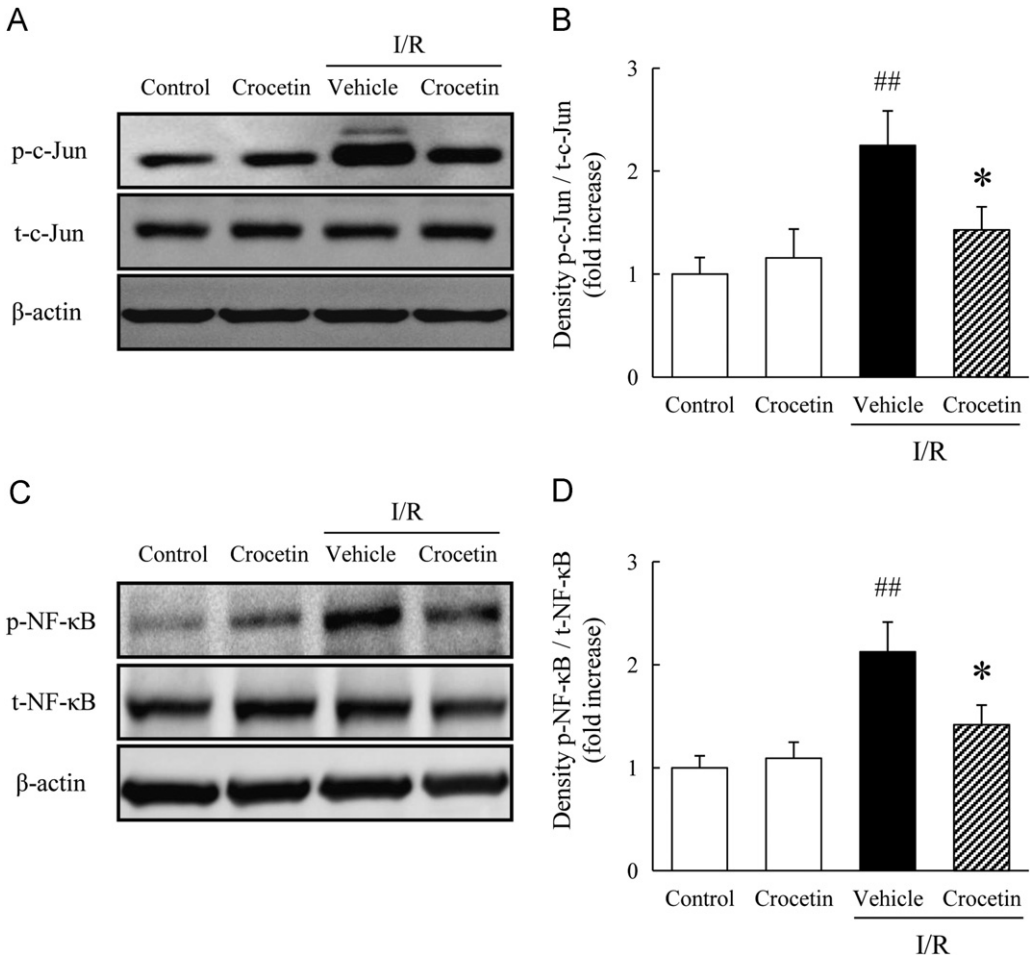

Fig. 8. Effects of crocetin on I/R-induced phosphorylation of inflammatory transcription factor in the mouse retina. (A) and (C) Representative band images for (A) c-Jun and (C) NF-κB in retinas treated with CMC, crocetin, I/R plus vehicle, or I/R plus crocetin. (B) and (D) Quantitative analysis of the band densities for (B) c-Jun and (D) NF-κB. Data are shown as means ± S.E.M. ($n=6$). $^{*}P<0.05$ vs. I/R plus vehicle (vehicle). $^{\#\#}P<0.01$ vs. CMC (control).

investigated the effects of crocetin on the activations of MAPKs induced by I/R. We found that crocetin significantly inhibited p38 and JNK activations, but not ERK 1/2 activation. These results suggest that I/R-induced reactive oxygen species may act upstream of activation of the p38 and JNK signaling cascade, and that in contrast, I/R-induced ERK 1/2 activation may be mediated by ROS-independent signaling pathways. Similarly, we previously reported that the free-radical scavenger edaravone inhibited the activations of p38 and JNK, but not that of ERK 1/2, seen in whole retinas after either light exposure (Imai et al., 2010) or intravitreal injection of NMDA (Inokuchi et al., 2009).

AP-1 and NF-κB are redox-sensitive as well as inflammatory transcription factors that play critical roles in neuronal cell death during in ischemic injury in both brain and retina (Karin et al., 2001; Dvoriantchikova et al., 2009; Crack et al., 2006). AP-1 is a complex that consists either of heterodimers of members of the Fos and Jun families of proteins or of homodimers of members of the Jun family of proteins (Hai and Curran, 1991). AP-1 is activated through JNK- and p38-induced phosphorylations of c-Jun and c-Fos (Roduit and Schorderet, 2008). In the present study, Western blot analysis demonstrated that c-Jun and NF-κB p65 were phosphorylated after I/R, and that administration of crocetin significantly reduced the I/R-induced activations of both c-Jun and NF-κB. Previously it has been shown that in vascular smooth muscle cells, the Ang II-induced mRNA expression of c-jun is decreased by crocetin (Zhou et al., 2010) and that in cultured rat brain microglial cells, crocetin reduces LPS-induced NF-κB activation (Nam et al., 2010). Antioxidants have also been shown to reduce the activations of c-Jun and NF-κB induced by ischemia (Wen et al., 2006; Qian et al., 2012). Taken together, these findings suggest that crocetin inhibits ischemic retinal damage by suppressions of NF-κB and AP-1 activities.

Ocular ischemic syndrome is the syndrome that results from chronic ocular hypoperfusion. According to our previous evaluation, ocular blood flow was maintained hypoperfusion from just after ligation of PPA and ECA to 5 h after ligation (Ogishima et al., 2011), and it is suggested that chronic hypoperfusion is persisted for an extended period because retinal vascular permeability was increased at 5 days after ligation and administration of ameliorants of ocular circulation from reperfusion showed inhibitory effect against increasing in retinal vascular permeability (data not shown). Moreover, this prolonged disturbance in the blood supply to the retina induces retinal dysfunction and histological damage, which were characterized as an ocular ischemic syndrome. Therefore, this animal model was used as a mouse model of ocular ischemic syndrome.

In conclusion, we have demonstrated in mice that oral administration of crocetin can inhibit I/R-induced retinal cell death, and we suggest that this effect of crocetin may be mediated partly by its antioxidant action. Taken together, the data now available indicate that crocetin has potential as a prophylactic agent for degenerative diseases of the retina, such as ocular ischemic syndromes.

References

Ahmad, A.S., Ansari, M.A., Ahmad, M., Saleem, S., Yousuf, S., Hoda, M.N., Islam, F., 2005. Neuroprotection by crocetin in a hemi-parkinsonian rat model. Pharmacol. Biochem. Behav. 81, 805–813.

Bucolo, C., Ward, K.W., Mazzon, E., Cuzzocrea, S., Drago, F., 2009. Protective effects of a coumarin derivative in diabetic rats. Invest. Ophthalmol. Vis. Sci. 50, 3846–3852.

Bucolo, C., Drago, F., 2011. Carbon monoxide and the eye: implications for glaucoma therapy. Pharmacol. Ther. 130, 191–201.

Bucolo, C., Leggio, G.M., Drago, F., Salomone, S., 2012. Eriodictyol prevents early retinal and plasma abnormalities in streptozotocin-induced diabetic rats. Biochem. Pharmacol. 84, 88–92.

Crack, P.J., Taylor, J.M., Ali, U., Mansell, A., Hertzog, P.J., 2006. Potential contribution of NF-κB in neuronal cell death in the glutathione peroxidase-1 knockout mouse in response to ischemia–reperfusion injury. Stroke 37, 1533–1538.

Daugeliene, L., Niwa, M., Hara, A., Matsuno, H., Yamamoto, T., Kitazawa, Y., Uematsu, T., 2000. Transient ischemic injury in the rat retina caused by thrombotic occlusion–thrombolytic reperfusion. Invest. Ophthalmol. Vis. Sci. 41, 2743–2747.

Dvoriantchikova, G., Barakat, D., Brambilla, R., Agudelo, C., Hernandez, E., Bethea, J.R., Shestopalov, V.I., Ivanov, D., 2009. Inactivation of astroglial NF-κB promotes survival of retinal neurons following ischemic injury. Eur. J. Neurosci. 30, 175–185.

Goldenberg-Cohen, N., Dadon, S., Avraham, B.C., Kramer, M., Hasanreisoglu, M., Eldar, I., Weinberger, D., Bahar, I., 2008. Molecular and histological changes following central retinal artery occlusion in a mouse model. Exp. Eye Res. 87, 327–333.

Grozdanic, S.D., Sakaguchi, D.S., Kwon, Y.H., Kardon, R.H., Sonea, I.M., 2003. Functional characterization of retina and optic nerve after acute ocular ischemia in rats. Invest. Ophthalmol. Vis. Sci. 44, 2597–2605.

Hai, T., Curran, T., 1991. Cross-family dimerization of transcription factors Fos/Jun and ATF/CREB alters DNA binding specificity. Proc. Nat. Acad. Sci. U.S.A. 88, 3720–3724.

Hosseinzadeh, H., Younesi, H.M., 2002. Antinociceptive and anti-inflammatory effects of *Crocus sativus* L. stigma and petal extracts in mice. BMC Pharmacol. 2, 7.

Ichi, T., Higashimura, Y., Katayama, T., Koda, T., Shimizu, T., Tada, M., 1995. Analysis of crocetin derivatives from gardenia (*Gardenia jasminoides* Ellis) fruits. J. Jpn. Soc. Food Sci. Technol.—Nippon Shokuhin Kagaku Kogaku Kaishi 42, 776–783.

Imai, S., Shimazawa, M., Nakanishi, T., Tsuruma, K., Hara, H., 2010. Calpain inhibitor protects cells against light-induced retinal degeneration. J. Pharmacol. Exp. Ther. 335, 645–652.

Inokuchi, Y., Imai, S., Nakajima, Y., Shimazawa, M., Aihara, M., Araie, M., Hara, H., 2009. Edaravone, a free radical scavenger, protects against retinal damage in vitro and in vivo. J. Pharmacol. Exp. Ther. 329, 687–698.

Karin, M., Takahashi, T., Kapahi, P., Delhase, M., Chen, Y., Makris, C., Rothwarf, D., Baud, V., Natoli, G., Guido, F., Li, N., 2001. Oxidative stress and gene expression: the AP-1 and NF-κB connections. Biofactors 15, 87–89.

Kloner, R.A., Przyklenk, K., Whittaker, P., 1989. Deleterious effects of oxygen radicals in ischemia/reperfusion. Resolved and unresolved issues. Circulation 80, 1115–1127.

Lelong, D.C., Bieche, I., Perez, E., Bigot, K., Leemput, J., Laurendeau, I., Vidaud, M., Jais, J.P., Menasche, M., Abitbol, M., 2007. Novel mouse model of monocular amaurosis fugax. Stroke 38, 3237–3244.

Li, N., Lin, G., Kwan, Y.W., Min, Z.D., 1999. Simultaneous quantification of five major biologically active ingredients of saffron by high-performance liquid chromatography. J. Chromatogr. A 849, 349–355.

Li, S.Y., Fu, Z.J., Ma, H., Jang, W.C., So, K.F., Wong, D., Lo, A.C., 2009. Effect of lutein on retinal neurons and oxidative stress in a model of acute retinal ischemia/reperfusion. Invest Ophthalmol. Vis. Sci. 50, 836–843.

Luo, Y., DeFranco, D.B., 2006. Opposing roles for ERK1/2 in neuronal oxidative toxicity. J. Biol. Chem. 281, 16436–16442.

Nam, K.N., Park, Y.M., Jung, H.J., Lee, J.Y., Min, B.D., Park, S.U., Jung, W.S., Cho, K.H., Park, J.H., Kang, I., Hong, J.W., Lee, E.H., 2010. Anti-inflammatory effects of crocin and crocetin in rat brain microglial cells. Eur. J. Pharmacol. 648, 110–116.

Ochiai, T., Shimeno, H., Mishima, K., Iwasaki, K., Fujiwara, M., Tanaka, H., Shoyama, Y., Toda, A., Eyanagi, R., Soeda, S., 2007. Protective effects of carotenoids from saffron on neuronal injury in vitro and in vivo. Biochim. Biophys. Acta 1770, 578–584.

Ogishima, H., Nakamura, S., Nakanishi, T., Imai, S., Kakino, M., Ishizuka, F., Tsuruma, K., Shimazawa, M., Hara, H., 2011. Ligation of the pterygopalatine and external carotid arteries induces ischemic damage in the murine retina. Invest. Ophthalmol. Vis. Sci. 52, 9710–9720.

Papandreou, M.A., Tsachaki, M., Efthimiopoulos, S., Cordopatis, P., Lamari, F.N., Margarity, M., 2011. Memory enhancing effects of saffron in aged mice are correlated with antioxidant protection. Behav. Brain Res. 219, 197–204.

Ohno, Y., Nakanishi, T., Umigai, N., Tsuruma, K., Shimazawa, M., Hara, H., 2012. Oral administration of crocetin prevents inner retinal damage induced by *N*-methyl-d-aspartate in mice. Eur. J. Pharmacol. 690, 84–89.

Qian, Y., Guan, T., Huang, M., Cao, L., Li, Y., Cheng, H., Jin, H., Yu, D., 2012. Neuroprotection by the soy isoflavone, genistein, via inhibition of mitochondria-dependent apoptosis pathways and reactive oxygen induced-NF-κB activation in a cerebral ischemia mouse model. Neurochem. Int. 60, 759–767.

Roduit, R., Schorderet, D.F., 2008. MAP kinase pathways in UV-induced apoptosis of retinal pigment epithelium ARPE19 cells. Apoptosis 13, 343–353.

Roth, S., Shaikh, A.R., Hennelly, M.M., Li, Q., Bindokas, V., Graham, C.E., 2003. Mitogen-activated protein kinases and retinal ischemia. Invest. Ophthalmol. Vis. Sci. 44, 5383–5395.

Selim, K., Tsimidou, M., Biliaderis, C.G., 2000. Kinetic studies of degradation of saffron carotenoids encapsulated in amorphous polymer matrices. Food Chem. 71, 199–206.

Shen, X.C., Qian, Z.Y., Wang, Y.J., Duan, J.A., 2009. Crocetin attenuates norepinephrine-induced cytotoxicity in primary cultured rat cardiac myocytes by antioxidant in vitro. J. Asian Nat. Prod. Res. 11, 417–425.

Shen, X.C., Qian, Z.Y., 2006. Effects of crocetin on antioxidant enzymatic activities in cardiac hypertrophy induced by norepinephrine in rats. Pharmazie 61, 348–352.

Tamaki, M., Kidoguchi, K., Mizobe, T., Koyama, J., Kondoh, T., Sakurai, T., Kohmura, E., Yokono, K., Umetani, K., 2006. Carotid artery occlusion and collateral circulation in C57Black/6 J mice detected by synchrotron radiation microangiography. Kobe J. Med. Sci. 52, 111–118.

Umigai, N., Tanaka, J., Tsuruma, K., Shimazawa, M., Hara, H., 2012. Crocetin, a carotenoid derivative, inhibits VEGF-induced angiogenesis via suppression of p38 phosphorylation. Curr. Neurovas. Res. 9, 102–109.

Wang, C.J., Lee, M.J., Chang, M.C., Lin, J.K., 1995. Inhibition of tumor promotion in benzo[*a*]pyrene-initiated CD-1 mouse skin by crocetin. Carcinogenesis 16, 187–191.

Wang, C.J., Hsu, J.D., Lin, J.K., 1991. Suppression of aflatoxin B_1-induced hepatotoxic lesions by crocetin (a natural carotenoid). Carcinogenesis 12, 1807–1810.

Watanabe, T., Terabe, S., 2000. Analysis of natural food pigments by capillary electrophoresis. J. Chromatogr. A 880, 311–322.

Wen, J., Watanabe, K., Ma, M., Yamaguchi, K., Tachikawa, H., Kodama, M., Aizawa, Y., 2006. Edaravone inhibits JNK-c-Jun pathway and restores anti-oxidative defense after ischemia–reperfusion injury in aged rats. Biol. Pharm. Bull. 29, 713–718.

Xia, Z., Dickens, M., Raingeaud, J., Davis, R.J., Greenberg, M.E., 1995. Opposing effects of ERK and JNK-p38 MAP kinases on apoptosis. Science 270, 1326–1331.

Xuan, B., Zhou, Y.H., Li, N., Min, Z.D., Chiou, G.C., 1999. Effects of crocin analogs on ocular blood flow and retinal function. J. Ocul. Pharmacol. Ther. 15, 143–152.

Yagi, K., Kitazato, K.T., Uno, M., Tada, Y., Kinouchi, T., Shimada, K., Nagahiro, S., 2009. Edaravone, a free radical scavenger, inhibits MMP-9-related brain hemorrhage in rats treated with tissue plasminogen activator. Stroke 40, 626–631.

Yamauchi, M., Tsuruma, K., Imai, S., Nakanishi, T., Umigai, N., Shimazawa, M., Hara, H., 2011. Crocetin prevents retinal degeneration induced by oxidative and endoplasmic reticulum stresses via inhibition of caspase activity. Eur. J. Pharmacol. 650, 110–119.

Yoshino, F., Yoshida, A., Umigai, N., Kubo, K., Lee, M.C., 2011. Crocetin reduces the oxidative stress induced reactive oxygen species in the stroke-prone spontaneously hypertensive rats (SHRSPs) brain. J. Clin. Biochem. Nutr. 49, 182–187.

Zhou, C.H., Xiang, M., He, S.Y., Qian, Z.Y., 2010. Protein kinase C pathway is involved in the inhibition by crocetin of vascular smooth muscle cells proliferation. Phytother. Res. 24, 1680–1686.